EXPERIMENTAL STUDY OF THE Fe-Si-C SYSTEM AND APPLICATION TO CARBON RICH EXOPLANETS

FRANCESCA MIOZZI FERRINI

Sorbonne Université, Institut de Minéralogie, de Physique des matériaux et de Cosmochimie, 4 Place Jussieu, 75005 Paris (F)

INTRODUCTION

Exoplanets currently represent one of the most vibrant topic of space sciences. Since the first exoplanets were discovered 20 years ago (Wolszczan & Frail, 1992; Mayor & Queloz, 1995;), the improvement in ground observational techniques and the launch of orbital missions as Kepler (Borucki *et al.*, 2010, 2011) and Tess (Stassun *et al.*, 2018) lead to the discovery of more than 4000 exoplanets, orbiting around stars with a wide variety of compositions.

Along with Sun-like stars, stars with a different chemical composition has been observed to host planetary systems. Within those, is remarkable to find stars enriched in carbon instead of oxygen (Bond *et al.*, 2010) as for example 55 Cancri (Delgado Mena *et al.*, 2010)

At the current state exoplanets are detected and studied through indirect methods that in many cases give access to the main properties of the planets, *i.e.* mass and radius (Lissauer & De Pater, 2013). These parameters are usually interpreted with models in which the mass and radius are calculated for a composition and internal structure decided a priori and displayed in the so-called M/R plots (*e.g.*, Duffy, 2015). At the current state, the majority of M/R plots are calculated for Earth-like planets or volatile enriched planets, due to the existing knowledge about the properties of the constituent minerals. However it is more difficult to calculate the mass radius plot for planets orbiting around stars with compositions very different from our Sun, as the physical properties at extreme conditions of the constituent minerals are sometimes unknown. An example are carbon enriched planets, they are considered to be mainly made by species in the Fe-Si-C system (*e.g.*, Madhusudhan *et al.*, 2012), as silicon and iron carbides. However the properties (*i.e.*, phase's relations, melting relations and melting temperature) of such ternary system, as well as the physical properties of some of the composing species at extreme conditions, were not widely investigated.

The aim of the present work was to investigate the ternary Fe-Si-C system and provide the parameters necessary to model carbon rich exoplanets interior. The project first focused on the binary Si-C system. In fact, unlike Fe-Si and Fe-C, Si-C is an uncommon system for Earth conditions and for such reason not well characterized at high pressure and temperature. Secondly Fe was added and experiments were performed on compositions belonging to the Fe-Si-C system.

METHODS

The scientific objective was pursued by performing experiments at extreme conditions of pressure and temperature, typically in the range between 20 and 200 GPa and 300-4000 K. *In situ* synchrotron X-ray diffraction and chemical analyses on the recovered samples, were used to obtain information about the properties of the compounds under extreme conditions. Diffraction experiments using Laser Heated Diamond Anvil Cell (LH-DAC) were performed on synchrotron beamlines (ESRF, Grenoble and Petra III, Hamburg), to determine phase relations and elastic properties. *Ex situ* analyses were performed to validate the *in situ* observations and to verify the existence of species that were not observed in diffraction analyses. In all the run, KCl was used as the pressure transmitting medium and pressure calibrant, using the equation of state from Dewaele *et al.* (2012) and the temperature correction from Campbell *et al.* (2009).

Samples were manufactures with physical vapour deposition (PVD) and ultra-rapid quench. Both techniques allowed to obtain thin layers (1-6 μm) of non-stoichiometric material with a desired composition. The chemistry of the obtained starting material was assessed with an electron microprobe analyser (EMPA).

Using PVD depositions as starting material for the experiments held a series of advantages. The deposited layer had constant thickness and homogeneous grain size. The nanometric size of the grains represented a great advantage for the experiments. As a matter of fact, the material was stable with an amorphous structure at ambient temperature, as a consequence the first phase to form during heating was the one thermodynamically favoured for the existing P-T conditions, thus avoiding major issues related to the kinetic. In the Si-C binary system three different compositions were investigated, whereas four compositions were used for the Fe-Si-C with different ratio of light elements.

Samples were recovered after the *in situ* diffraction experiment and a transverse cut of the heating spot was exposed with a broad ion beam and polished with a focused ion beam (FIB). For all the samples chemical and textural analyses were carried on with a scanning electron microscope (SEM).

The volumes obtained at high pressure and temperature for each phase were used to refine the equation of state and thermal model. First the ambient temperature data were refined with a Birch Murnaghan or a Vinet formalism. Successively also the data at high temperature were considered and the Mie Grüneisen Debye (MGD) or Thermal Pressure (TP) formalisms were employed (Miozzi *et al.*, 2018). The phase relations and melting curves were used to describe the evolution of the Fe-Si-C system in the P-T-X space.

Si-C SYSTEM

Silicon carbide (SiC) is the main phase in the Si-C system. Of the many stable polymorphs the cubic (3C) and hexagonal (6H) have been the most studied, also due to their occurrence in natural contexts, from grains in meteorites to inclusions.

In all the experimental run performed for this study, the amorphous starting material crystallize as cubic SiC in all the pressure range.

Cubic (3C) SiC display a zinc blende (B3) structure at low pressure and is known to undergo a phase transitions to a rock salt (B1) structure at high pressure, driven by a change in the coordination of the atoms, from tetrahedral to octahedral. The transition determine an important volume reduction. The pressure at which the phase transition occurs, was investigated by the mean of static and dynamic experiments and computations (*e.g.*, Sekine & Kobayashi, 1997; Zhuravlev *et al.*, 2013; Daviau & Lee, 2017).

Shock experiments studies located the transition at higher pressure with respect to static experiments. According to the pioneering experimental study of Yoshida *et al.* (1993), the phase transition takes place at 100 GPa under ambient temperature, whereas different computational studies indicate a pressure range between 60 and 80 GPa (Thakore *et al.*, 2013). The latter value is also supported by the experimental work by Daviau & Lee (2017), which located the phase transition between 60 and 70 GPa. We also note that the complete transition is not described in this study. The latest report by Kidokoro *et al.* (2017) is based on a rescaling of calculations made by Catti (2011) and advocates for a higher transition pressure. Pressure-volume-temperature EoS was only determined for the low pressure structure (Nisr *et al.*, 2017), whereas for the high pressure structure only a pressure-volume EoS between 60 and 90 GPa was reported (Kidokoro *et al.*, 2017). In the present study, the non-stoichiometry of the starting material determine the crystallization of SiC + C in carbon enriched samples, and SiC + Si in silicon enriched samples, thus enabling to determine the properties of stoichiometric SiC, as well as the phase diagram. The fine recrystallization of the material enables to individuate the peaks of each phase and follow the evolution of the phase transition. Many patterns displaying the coexistence of the two phases were collected, thus enabling to precisely determine the transition pressure (Fig. 1).

The pressure-volume-temperature equations of state were determined for both the structures. Fit to the data with the TP model yields better residuals in pressure (*i.e.,* smaller difference between actual measurements and pressure given by the EoS). The value of the Einstein temperature was fixed to that calculated from the

Debye temperature of the MGD model ($\theta^E = \theta^D * 0.806$). The obtained parameters for the zinc-blende B3 structure are $K_0 = 224 \pm 2$ GPa and $K_0' = 4.08 \pm 0.2$ with $\alpha_V = 0.62 \ 10^{-5} \pm 0.1$ K^{-1}. The latter is lower than previous experimental determination by Nisr *et al.* (2017) but is close the values derived from calculations by Varshney *et al.* (2015). The compressibility and pressure derivative have the same values as in the Birch-Murnaghan 300 K EoS with smaller errors on the parameters, whereas the values found with the thermal MGD model are slightly different. The isotherms well account for the entire data set with a χ 2 of 0.70.
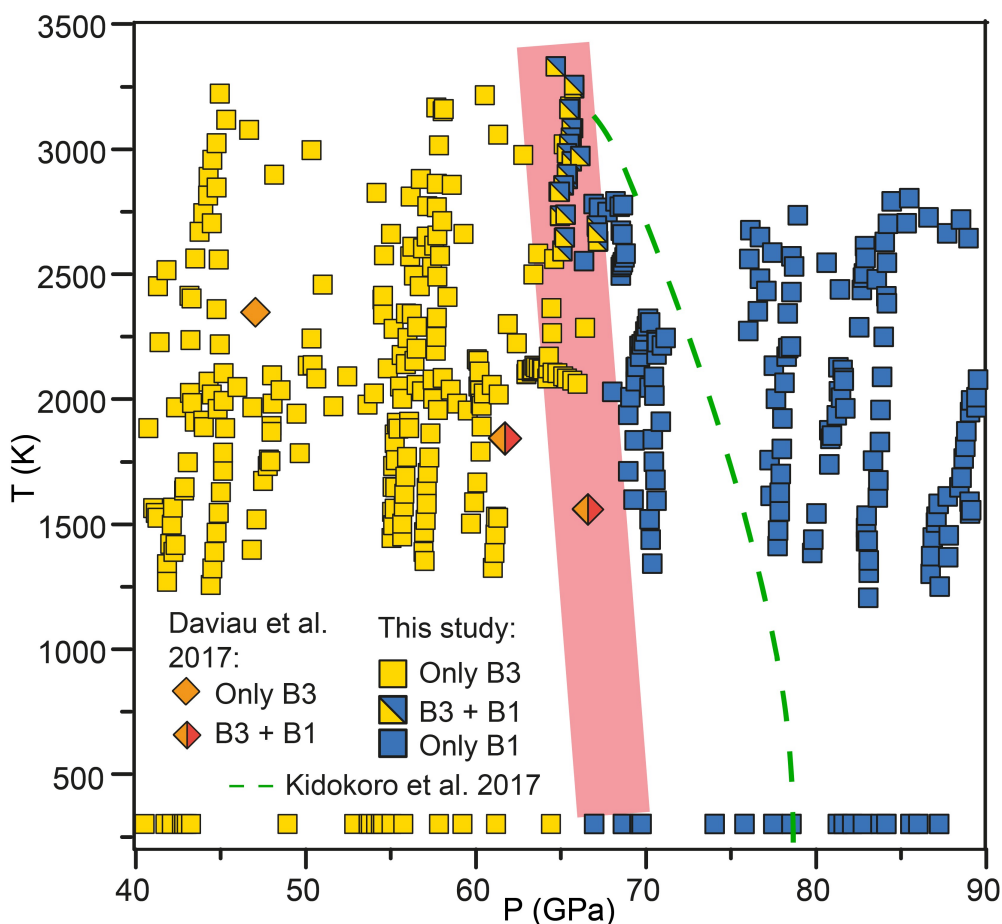

Fig. 1 - P-T phase diagram showing the data collected in the present study at pressure between 40 and 90 GPa and temperatures between 300-3500 K. SiC B3 and B1 are reported in different colours; the phase transition region is highlighted by the light red band. Diamonds illustrate the data from Daviau & Lee (2017). The green dashed line is the slope showed in Kidokoro *et al.* (2017) obtained after a rescaling of results by (Catti, 2001). From Miozzi *et al.* (2018).

In the stability field of the high-pressure rock-salt (B1) structure, 348 points were used to refine the thermal EoS, over a pressure range between 65 and 205 GPa and temperatures between 300 and 3000 K. In the TP thermal model refinement, the Einsten temperature was calculated from the Debye temperature and kept fixed to the value reported by Varshney *et al.* (2015), and the reference pressure is considered equal to zero. As a standard procedure for the fit, we first refined only γ_0 and q using the V_0, K_0, and K_0' obtained with the EoS at 300 K. Then, for the final processing cycle, also the value of V_0, K_0, and K_0' were refined together with the other parameters of the thermal model.

The obtained results are $V_0 = 65.9 \pm 0.04$ Å^3, $K_0 = 339 \pm 2$ GPa, $K_0' = 3.03 \pm 0.02$, and $\alpha = 0.58 \times 10^{-5} \pm 0.01$ K^{-1} with the Einstein temperature calculated from of the Debye temperature of B1 structure. The refined values for V_0, K_0, and K_0' are the same as for the MGD model within error bars, and χ^2 = 2.67. The coefficient of thermal expansion falls within the range of values derived from theoretical models (Varshney *et al.*, 2015) which also predicted a significant decrease across the transition from the B3 to the B1 structure.

The non-stoichiometry of the starting materials also provided the ideal frame to study the Si-C binary phase diagram (Miozzi *et al.*, 2018). With silicon enriched starting material SiC + Si was the stable assemblage in all the pressure range. A melting point was observed at 2100 K and 60 GPa using the disappearance of the solid diffraction peaks and a plateau in the temperature *vs.* power as a criteria for melting. In the quenched assemblage SiC + Si were observed as the stable phases. On the carbon enriched side the assemblage SiC + C was stable above all the pressure and temperature range and melting was never observed.

Fe-Si-C SYSTEM

Two of the fundamental characteristics that are necessary to determine in multi elemental systems are the eutectic melting curve and the composition of the eutectic. In this frame, the properties of the Fe-Si-C systems at high pressure and temperature are widely unknown, as studies were only performed at ambient pressure and moderate temperature with application to material sciences. Nevertheless, an initial idea of the behaviour of the system can be extrapolated from the behaviour of the Fe-C and Fe-Si both widely characterised at high pressure and temperature due to their importance for the Earth's interior.

In the Fe-C system Fe_3C and Fe_7C_3 are the main components. The system has a low melting temperature (Morard *et al.*, 2017) compared to pure iron (Anzellini *et al.*, 2013) and a constant eutectic composition upon P increase (Mashino *et al.*, 2019). Silicon on the other hand has a negligible effect on the melting temperature of pure iron up to 18 at % (Fischer *et al.*, 2013), whereas the silicon content at the eutectic drastically change with pressure (Ozawa *et al.*, 2016). Using the binary Fe-C, Fe-Si from literature and the previously determined Si-C as a reference, we proceeded with the reconstruction of the phase relations in the ternary Fe-Si-C diagram (Fig. 2)

The four investigated compositions display different stable mineralogical assemblages, consistent with the increment in the light elements content of the starting material.

For the starting material with lower light elements content ($FeSi_3C_3$) the stable phases were hcp Fe + Fe_3C in all the pressure range. Hcp Fe is the first phase to form and the solidus phase, with Fe_3C disappearing at the eutectic temperature. The determined melting curve display an evolution in T consistent with the binary Fe-C. The V-P plot of hcp Fe compared to literature data display an increment of the volume in all the pressure range. Such increment can't be related with the sole presence of silicon inside the structure. It has in fact been observed by Edmund *et al.* (2019) that hcp Fe can host up to 8 at % without showing an increase of the volume. As according to the lever rule our sample should host a maximum amount of 3 at % Si, the observed volume shift in the present data should be a consequence of the simultaneous incorporation of carbon together with silicon. Moreover, the latter is known for being in substitution while carbon can occupy the interstitial positions in the unit cell (Caracas, 2017), thus confirming carbon incorporation as the cause of the observed volume increment. The use of PVD depositions as starting material allowed to obtain finely recrystallized diffraction patterns of the molten sample that were used to determine the composition of the liquid with a Rietveld refinement. As silicon is in solution in iron the composition was assumed considering a 1:1 partition between the solid and the liquid. For carbon the recovered value served just as a lower bound as part of the carbon is in solution in iron as well. We considered as composition of the ternary eutectic a value of 3 at % Si and 13 at % C.

Increasing the light elements content ($FeSi_6C_5$) contribute to stabilise FeSi in coexistence with multiple iron carbides. The determined melting curve is higher in T compared to the one obtained for $FeSi_3C_3$ and plot between the curves corresponding to the Fe-Si and Fe-C systems. A further increase in the light elements content ($FeSi_{10}C_{20}$) corresponds to the existence of FeSi as only stable phase below 110 GPa and the exsolution of Fe_7C_3 above such pressure. Furthermore, in the transverse cut of the samples diamonds were observed in coexistence with the stable phases. It hadn't been possible to notice their presence in the diffraction patterns due to the overlap of the iron carbides peaks with the diamond's ones. The melting curve is consistent with the one retrieved for $FeSi_6C_5$. Finally FeSi + Fe_7C_3 are stable upon all the pressure range in the sample with higher light

elements content ($FeSi_{20}C_{10}$). The melting curve is consistent with the two previous compositions and diamonds are observed in the transverse cut as well.
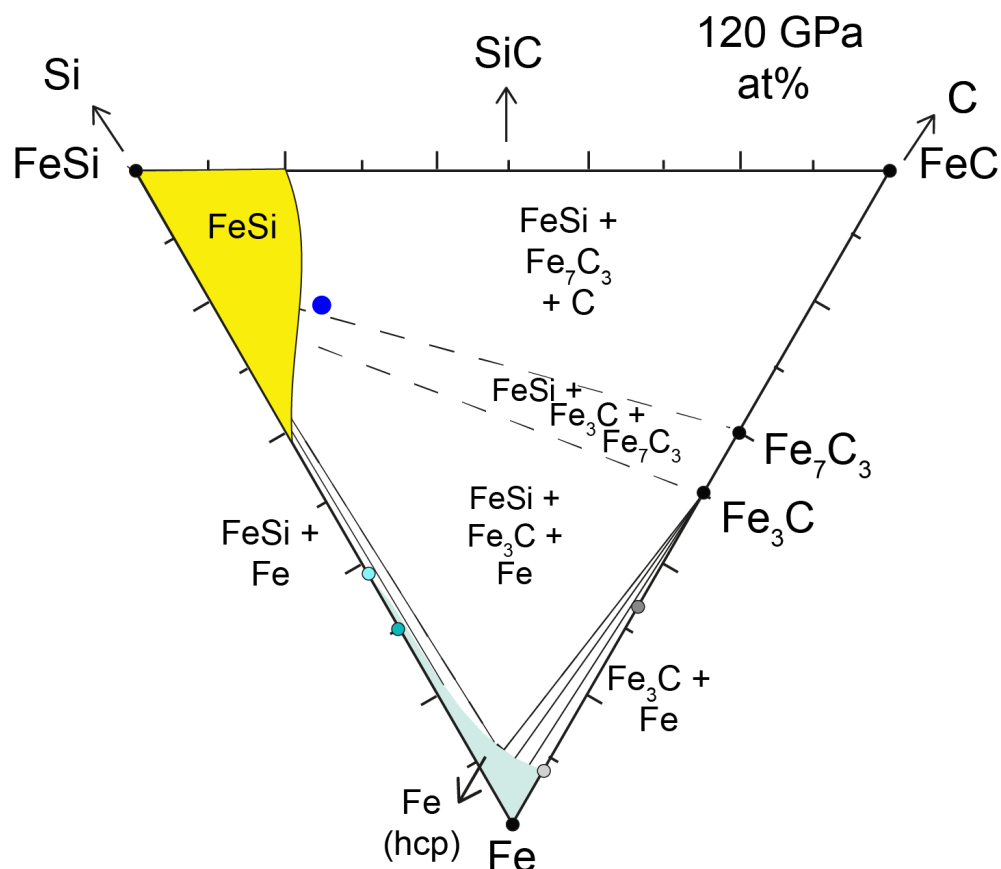

Fig. 2 - Isothermal and isobaric section of the Fe-Si-C system. The phases stable in subsolidus are shown. The solubility of silicon and carbon into Hcp Fe and in FeSi determine the existence of the two solubility field on the two Fe and FeSi corners. Moving from the iron rich corner toward the Si-C side the stable mineral assemblage is enriched in carbon.

All the observed properties permitted to reconstruct the evolution in pressure and temperature of the ternary Fe-Si-C diagram. The higher melting temperature of the samples with a high light elements content (*i.e.*, 2500 K at 50 GPa for $FeSi_6C_5$, $FeSi_{10}C_{20}$ and $FeSi_{20}C_{10}$), compared to the one of $FeSi_3C_3$ (*i.e.*, 2300 K at 50 GPa) implies the existence of a second minimum in the ternary system potentially corresponding to a peritectic point. This observation is consistent with the observations made for the Fe-C system where two peritectic points are predicted to exist in the carbon rich side of the diagram (Lord *et al.*, 2009).

Finally, the P-V-T data sets collected for all the stable phases permit the determination of the thermal equations of state. The addition of carbon in solution in both hcp Fe and FeSi seems to induce a change in the phases' thermal behaviour at high pressure worthy of further investigations.

APPLICATION TO EXOPLANETS INTERIOR

The obtained results offer new insight into carbon rich exoplanets interior and provide the data to make preliminary models of carbon rich exoplanets interior.

The phase relations established for the ternary system provide an overview on how compositional variations would affect the crystallization processes of a Fe-Si-C core and the outcomes in terms of structures and dynamic hence the likelihood of starting a dynamo and a magnetic field. The presence of a metallic core and its main characteristics, in fact, deeply affect the properties of a planet by determining the possibility to start convection. If during core formation a buoyant chemical component is released, a compositional convection can

be activated, thus starting a dynamo and consequently a magnetic field. The existence of a magnetic field is one of the requirements needed for a planet to be consider as habitable, as it prevents the atmosphere to be eroded by stellar winds (Lammer *et al.*, 2009).

In the ternary Fe-Si-C system, the diversity of the mineralogical assemblages stable in each portion of the phase diagram implies the existence of different crystallization scenarios, from *i)* a bottom-up crystallization style, with denser iron crystals that form and sink toward the bottom part of the forming core, to *ii)* a top-down solidification style, if iron carbides are the first phase to crystallize. In this two scenarios only the first is consider to potentially activate a dynamo. Finally, is noteworthy that solidifying a core in the FeSi enriched side of the diagram would represent an anomaly compared to the mechanisms proposed for the formation of some solar system's planets. The almost negligible density contrast of the solid and liquid would lead to the crystallization of a mushy layer.

The data obtained on the binary Si-C system were used to investigate if the volume jump induced by the phase transition would affect the dynamic of an SiC mantle (Miozzi *et al.*, 2018). The results display how the phase transition would not affect the possibility of having convection, however starting a convection would need a higher activation energy compared to a Earth-like mantle.

Furthermore, the equations of state for SiC were used to determine the mass radius plots for two archetypal carbon enriched planets (Fig. 3).
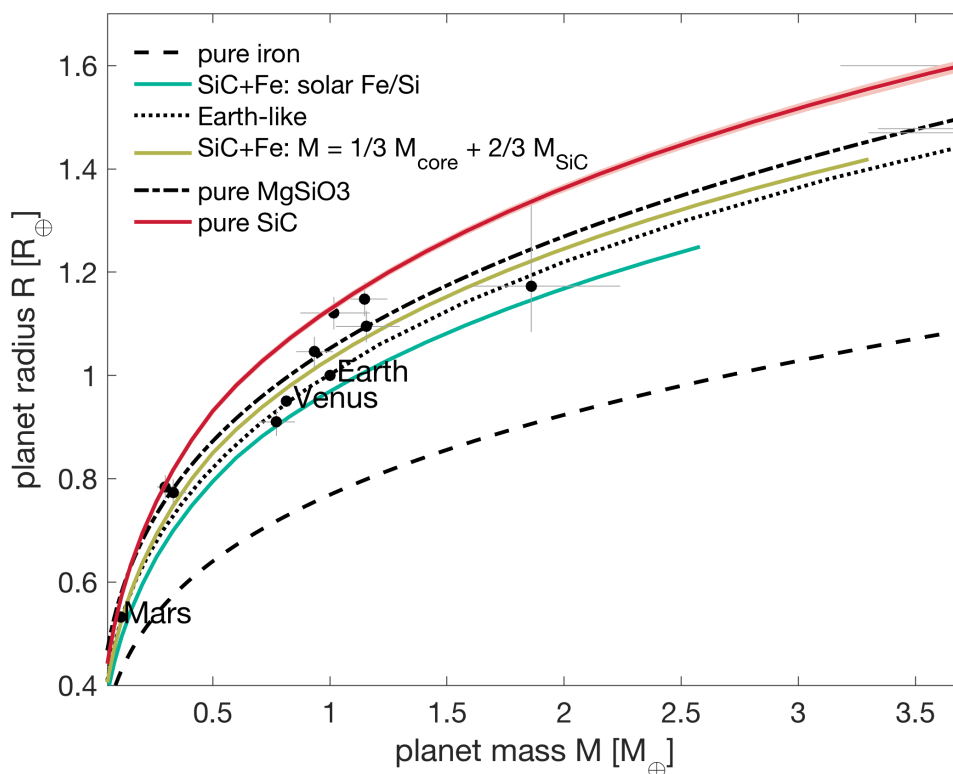

Fig. 3 - Mass radius relations for different idealized exoplanet interiors together with the standard comparison curves (pure Fe, MgSiO$_3$ and Earth-like). Several C-rich end-members are proposed: a pure SiC planet, a core + SiC mantle planet with mass proportions similar to the Earth's core and mantle, and finally, an iron core + SiC mantle planet with a bulk ratio of Fe/Si that matches solar abundances. The black dots show the measured masses and radii for solar system planets and some observed exoplanets. From Miozzi *et al.* (2018)

For both models a pure iron core was assumed in order to follow the assumptions commonly used in the exoplanets community (Wang *et al.*, 2019). In the first model, the c-rich planet has an Earth-like structure, the iron core makes up for a third of the planet mass and the rest is considered as made by SiC. In the second model, the proportions of Fe and SiC are chosen so as the bulk composition of the planet match the solar Fe/Si

abundances (solar Fe/Si; Lodders, 2003). Extrapolations have been limited to 3.5 times the mass of the Earth for the 1/3 Fe core planet and 2.5 times the mass of the Earth for the solar Fe/Si ratio planet. As expected, the addition of iron to SiC contribute to increase the average density of the planet, with the curve for the solar Fe/Si plotting sensibly below the Earth-like curve. On the other hand, the Earth-like SiC planet displays an intermediate density between pure SiC and the solar Fe/Si, and is close to the M/R plot of the Earth. This modelling confirms that it is impossible (or difficult) to discriminate between an Earth like planet and a carbon enriched planet just from the mass/radius systematics, thus stressing the need for additional constraints for the interpretation of observational data and a better identification of the nature of such planets.

It is important to notice that our carbon rich idealized planet is unlikely to occur in nature as Mg and O are expected to be present in exoplanets (Carter-Bond *et al.*, 2012). Mg-O free end-members are important to provide limits on the bulk density and interpret possible interiors of observed exoplanets. However, neglecting Mg and O underestimate the mineralogical complexity of the forming planet, the potential effect on dynamic and ultimately habitability.

This work wants to represent a first step in the investigation of planetary variability. Hopefully it can contribute to understand this new worlds and drive the attention toward a collaborative approach between geosciences and astronomy.

ACKNOWLEDGEMENTS

REFERENCES

Anzellini, S., Dewaele, A., Mezouar, M., Loubeyre, P., Morard, G (2013): Melting of iron at Earth's inner core boundary based on fast X-ray diffraction. *Science*, **340**, 464–466.

Bond, J.C., O'Brien, D.P., Lauretta, D.S. (2010): The compositional diversity of extrasolar terrestrial planets. I. In situ simulations. *Astrophys. J.,* **715**, 1050–1070.

Borucki, W.J., Koch, D., Basri, G., Batalha, N., Brown, T., Caldwell, D., Caldwell, J., Christensen-Dalsgaard, J., Cochran, W.D., DeVore, E., Dunham, E.W., Dupree, A.K., Gautier, T.N., Geary, J.C., Gilliland, R., Gould, A., Howell, S.B., Jenkins, J.M., Kondo, Y., Latham, D.W., Marcy, G.W., Meibom, S., Kjeldsen, H., Lissauer, J.J., Monet, D.G., Morrison, D., Sasselov, D., Tarter, J., Boss, A., Brownlee, D., Owen, T., Buzasi, D., Charbonneau, D., Doyle, L., Fortney, J., Ford, E.B., Holman, M.J., Seager, S., Steffen, J.H., Welsh, W.F., Rowe, J., Anderson, H., Buchhave, L., Ciardi, D., Walkowicz, L., Sherry, W., Horch, E., Isaacson, H., Everett, M.E., Fischer, D., Torres, G., Johnson, J.A., Endl, M., MacQueen, P., Bryson, S.T., Dotson, J., Haas, M., Kolodziejczak, J., Van Cleve, J., Chandrasekaran, H., Twicken, J.D., Quintana, E. V., Clarke, B.D., Allen, C., Li, J., Wu, H., Tenenbaum, P., Verner, E., Bruhweiler, F., Barnes, J., Prsa, A. (2010): Kepler Planet-Detection Mission: Introduction and First Results. *Science*, **80**, 327, 977–980.

Borucki, W.J., Koch, D.G., Basri, G., Batalha, N., Boss, A., Brown, T.M., Caldwell, D., Christensen-Dalsgaard, J., Cochran, W.D., Devore, E., Dunham, E.W., Dupree, A.K., Gautier, T.N., Geary, J.C., Gilliland, R., Gould, A., Howell, S.B., Jenkins, J.M., Kjeldsen, H., Latham, D.W., Lissauer, J.J., Marcy, G.W., Monet, D.G., Sasselov, D., Tarter, J., Charbonneau, D., Doyle, L., Ford, E.B., Fortney, J., Holman, M.J., Seager, S., Steffen, J.H., Welsh, W.F., Allen, C., Bryson, S.T., Buchhave, L., Chandrasekaran, H., Christiansen, J.L., Ciardi, D., Clarke, B.D., Dotson, J.L., Endl, M., Fischer, D., Fressin, F., Haas, M., Horch, E., Howard, A., Isaacson, H., Kolodziejczak, J., Li, J., Macqueen, P., Meibom, S., Prsa, A., Quintana, E. V., Rowe, J., Sherry, W., Tenenbaum, P., Torres, G., Twicken, J.D., Van Cleve, J., Walkowicz, L., Wu, H. (2011): Characteristics of Kepler planetary candidates based on the first data set. *Astrophys. J.,* **728**, 117.

Campbell, A.J., Danielson, L., Righter, K., Seagle, C.T., Wang, Y., Prakapenka, V.B. (2009): High pressure effects on the iron-iron oxide and nickel-nickel oxide oxygen fugacity buffers. *Earth Planet. Sci. Lett.*, **286**, 556–564.

Caracas, R. (2017): The influence of carbon on the seismic properties of solid iron. *Geophys. Res. Lett.*, **44**, 128–134.

Carter-Bond, J.C., O'Brien, D.P., Raymond, S.N. (2012). The compositional diversity of extrasolar terrestrial planets. II. Migration simulations. *Astrophys. J.*, **760**, 44.

Catti, M. (2001): Orthorhombic intermediate state in the zinc blende to rocksalt transformation path of SiC at high pressure.

Phys. Rev. Lett., **87**, 035504.

Daviau, K. & Lee, K.K.M. (2017): Zinc-blende to rocksalt transition in SiC in a laser-heated diamond-anvil cell. *Phys. Rev. B*, 95, 1–6.

Delgado Mena, E., Israelian, G., González Hernández, J.I., Bond, J.C., Santos, N.C., Udry, S., Mayor, M. (2010): Chemical clues on the formation of planetary systems: C/O versus Mg/Si for HARPS GTO sample. *Astrophys. J.*, **725**, 2349–2358.

Dewaele, A., Belonoshko, A.B., Garbarino, G., Occelli, F., Bouvier, P., Hanfland, M., Mezouar, M. (2012): High-pressure–high-temperature equation of state of KCl and KBr. *Phys. Rev. B*, **85**, 214105.

Duffy, T., Madhusudhan, N., Lee, K.K.M. (2015): Mineralogy of Super-Earth Planets. In: "Treatise on Geophysics", G. Schubert Ed., Elsevier, Amsterdam (The Netherlands), 149-178.

Edmund, E., Antonangeli, D., Decremps, F., Miozzi, F., Morard, G., Boulard, E., Clark, A.N., Ayrinhac, S., Gauthier, M., Morand, M., Mezouar, M. (2019): Velocity-density systematics of Fe-5wt%Si: constraints on Si content in the Earth's inner core. *J. Geophys. Res.-Solid Ea.rth*.

Fischer, R.A., Campbell, A.J., Reaman, D.M., Miller, N.A., Heinz, D.L., Dera, P., Prakapenka, V.B. (2013): Phase relations in the Fe-FeSi system at high pressures and temperatures. *Earth Planet. Sci. Lett.*, **373**, 54–64.

Kidokoro, Y., Umemoto, K., Hirose, K., Ohishi, Y. (2017): Phase transition in SiC from zinc-blende to rock-salt structure and implications for carbon-rich extrasolar planets. *Am. Mineral.*, **102**, 2230–2234.

Lammer, H., Bredehöft, J.H., Coustenis, A., Khodachenko, M.L., Kaltenegger, L., Grasset, O., Prieur, D., Raulin, F., Ehrenfreund, P., Yamauchi, M., Wahlund, J.-E., Grießmeier, J.-M., Stangl, G., Cockell, C.S., Kulikov, Y.N., Grenfell, J.L., Rauer, H. (2009): What makes a planet habitable? *Astron. Astrophys. Rev.*, **17**, 181–249.

Lissauer, J.J. & De Pater, I. (2013): Fundamental planetary science: physics, chemistry and habitability. Cambridge University Press, New York (USA), 595 p.

Lodders, K. (2003): Solar System Abundances and Condensation Temperatures of the Elements. *Astrophys. J.*, **591**, 1220–1247.

Lord, O.T., Walter, M.J., Dasgupta, R., Walker, D., Clark, S.M. (2009): Melting in the Fe-C system to 70 GPa. *Earth Planet. Sci. Lett.*, **284**, 157–167.

Madhusudhan, N., Lee, K.K.M., Mousis, O. (2012): A possible carbon-rich interior in super-Earth 55 Cancri e. *Astrophys. J.* **759**, L40.

Mashino, I., Miozzi, F., Hirose, K., Morard, G., Sinmyo, R. (2019): Melting experiments on the Fe-C binary system up to 255 GPa: Constraints on the carbon content in the Earth's core. *Earth Planet. Sci. Lett.*, **515**, 135–144.

Mayor, M. & Queloz, D. (1995): A Jupiter-mass companion to a solar-type star. *Nature,* **378**, 355–359.

Miozzi, F., Morard, G., Antonangeli, D., Clark, A.N., Mezouar, M., Dorn, C., Rozel, A., Fiquet, G. (2018): Equation of state of SiC at extreme conditions: new insight into the interior of carbon-rich exoplanets. *J. Geophys. Res.-Planet.*, **19**, 2295–2309.

Morard, G., Andrault, D., Antonangeli, D., Nakajima, Y., Auzende, A.L., Boulard, E., Cervera, S., Clark, A., Lord, O.T., Siebert, J., Svitlyk, V., Garbarino, G., Mezouar, M. (2017): Fe–FeO and Fe–Fe3C melting relations at Earth's core–mantle boundary conditions: Implications for a volatile-rich or oxygen-rich core. *Earth Planet. Sci. Lett.*, **473**, 94–103.

Nisr, C., Meng, Y., MacDowell, A.A., Yan, J., Prakapenka, V., Shim, S.-H. (2017): Thermal expansion of SiC at high pressure-temperature and implications for thermal convection in the deep interiors of carbide exoplanets. *J. Geophys. Res.-Planet.*, 122, 124–133.

Ozawa, H., Hirose, K., Yonemitsu, K., Ohishi, Y. (2016): High-pressure melting experiments on Fe-Si alloys and implications for silicon as a light element in the core. *Earth Planet. Sci. Lett.*, **456**, 47–54.

Sekine, T. & Kobayashi, T. (1997): Shock compression of 6H polytype SiC to 160 GPa. *Phys. Rev. B*, **55**, 8034–8037.

Stassun, K.G., Oelkers, R.J., Pepper, J., Paegert, M., Lee, N. De, Torres, G., Latham, D.W., Charpinet, S., Dressing, C.D., Huber, D., Kane, S.R., Lépine, S., Mann, A., Muirhead, P.S., Rojas-Ayala, B., Silvotti, R., Fleming, S.W., Levine, A., Plavchan, P. (2018): The TESS Input Catalog and Candidate Target List. *Astron. J.,* **156**, 102.

Thakore, B.Y., Khambholja, S.G., Vahora, A.Y., Bhatt, N.K., Jani, A.R. (2013): Thermodynamic properties of 3C—SiC. *Chinese Phys. B*, **22**, 106401.

Varshney, D., Shriya, S., Varshney, M., Singh, N., Khenata, R. (2015): Elastic and thermodynamical properties of cubic (3C) silicon carbide under high pressure and high temperature. *J. Theor. Appl. Phys.*, **9**, 221–249.

Wang, H.S., Liu, F., Ireland, T.R., Brasser, R., Yong, D., Lineweaver, C.H. (2019): Enhanced constraints on the interior composition and structure of terrestrial exoplanets. *Mon. Not. R. Astron. Soc.*, **482**, 2222–2233.

Wolszczan, A. & Frail, D.A. (1992): A planetary system around the millisecond pulsar PSR1257 + 12. *Nature,* **355**, 145–147.

Yoshida, M., Onodera, A., Ueno, M., Takemura, K., Shimomura, O. (1993): Pressure-induced phase transition in SiC. *Phys.*

Rev. B, **48**, 10587–10590.

Zhuravlev, K.K., Goncharov, A.F., Tkachev, S.N., Dera, P., Prakapenka, V.B. (2013): Vibrational, elastic, and structural properties of cubic silicon carbide under pressure up to 75 GPa: Implication for a primary pressure scale. *J. Appl. Phys.*, **113**, 113503.